Heliyon 9 (2023) e20248

Contents lists available at ScienceDirect

Heliyon

journal homepage: www.cell.com/heliyon

Bone-homing metastatic breast cancer cells impair osteocytes' mechanoresponse in a 3D loading model

Blayne A. Sarazin [a], Boyuan Liu [a], Elaine Goldman [a], Ashlyn N. Whitefield [a], Maureen E. Lynch [a,b,*]

[a] Department of Mechanical Engineering, University of Colorado, Boulder, CO, 80309, USA
[b] BioFrontiers Institute, University of Colorado, Boulder, CO, 80309, USA

ARTICLE INFO

Keywords:
Breast cancer
Bone metastasis
3D models
Osteocyte
Mechanobiology

ABSTRACT

Breast cancer predominantly metastasizes to the skeleton. Mechanical loading is reliably anabolic in bone, and also inhibits bone metastatic tumor formation and bone loss in vivo. To study the underlying mechanisms, we developed a 3D culture model for osteocytes, the primary bone mechanosensor. We verified that MLO-Y4s responded to perfusion by reducing their *rankl* and *rankl:opg* gene expression. We next cultured MLO-Y4s with tumor-conditioned media (TCM) collected from human breast cancer cells (MDA-MB-231s) and a corresponding bone-homing subclone to test the impacts on osteocytes' mechanosensation. We found that TCM from the bone-homing subclone was more detrimental to MLO-Y4 growth and viability, and it abrogated loading-induced changes to *rankl:opg*. Our studies demonstrate that MLO-Y4s, including their mechanoresponse to perfusion, were more negatively impacted by soluble factors from bone-homing breast cancer cells compared to those from parental cells.

1. Introduction

Bone fractures and other skeletal-related events (SREs) are common, life-threatening complications of bone metastases, and are a serious clinical challenge in the management of metastatic breast cancer. For breast cancer, bone is the predominant distant metastatic site [1]. Breast cancer bone metastasis induces bone disease through accelerated bone loss, heightened fragility, and risk for suffering an SRE. SREs (e.g., severe pain, fracture), which are most numerous in breast cancer, increase the risk for subsequent SREs (as many as four per year [2]) and early death on the order of weeks [3]. The current view of osteolytic tumor-induced bone disease (TIBD) is that tumor cells stimulate osteoblasts to increase osteoclast differentiation and resorption activity, leading to a vicious cycle of bone loss. However, osteocytes (OCys) are involved in bone metastasis as well, as they are specialized sensory bone cells that function as "managers" to sense and integrate physiochemical signals to appropriately coordinate bone tissue remodeling [4,5]. In the current study, we investigated how bone metastatic breast cancer alters OCys' mechanosensing function and the downstream impacts on bone remodeling signals.

Increased mechanical stimuli, which are well-documented to increase bone and mitigate bone loss due to myriad pathologies (e.g., aging [6]), may also be protective against TIBD with concomitant anti-tumorigenic effects. A few promising reports indicated that

* Corresponding author. Department of Mechanical Engineering University of Colorado 427 UCB, Boulder, CO, 80309, USA.
E-mail address: Maureen.Lynch@colorado.edu (M.E. Lynch).
@LynchLab (M.E. Lynch)

https://doi.org/10.1016/j.heliyon.2023.e20248
Received 8 May 2023; Received in revised form 23 June 2023; Accepted 14 September 2023
Available online 21 September 2023

exercise reduced bone loss in breast cancer survivors [7,8] and induced positive physical outcomes (e.g., lower fatigue) in patients with existing bone metastases without SREs [9–11]. In preclinical studies, increased mechanical stimuli inhibited both metastatic tumor formation and bone loss in breast [12,13] and multiple myeloma [14,15] bone metastases. Specifically in breast cancer, tibial compression applied to a mouse model of breast cancer bone metastasis protected against bone loss and tumor formation [13], but pathologicallyhigh loading appeared to accelerate metastasis [12], highlighting the need to better understand the impacts of loading on TIBD.

Recently, OCys have been definitively implicated in TIBD. Increased lesions, osteoclast formation, and bone loss in late-stage multiple myeloma patients were correlated with increased OCy apoptosis and circulating levels of DKK1 and sclerostin [16,17]. Now, they are established as important cellular players in TIBD, but their role remains under investigation. Because OCys are the primary regulators of mechanically-regulated bone homeostasis and OCy dysfunction is a feature in many skeletal pathologies that lead to bone fragility [4,5], we broadly hypothesize that bone metastatic breast cancer cells impair osteocyte function, which would be a new mechanism of TIBD.

While many mechanistic studies have investigated how OCys, particularly mechanically-stimulated OCys, modulate tumor cell viability and behavior, such as motility [12,18,19], few have studied how OCys are reciprocally impacted by tumor cells. In vivo, the OCy lacunar-canalicuar network was disrupted by both multiple myeloma [20] and melanoma bone metastasis [21] during TIBD development. Further, upon direct contact with multiple myeloma cells in vivo, OCys underwent apoptosis and subsequently expressed greater RANKL and sclerostin than control mice, which contributes to bone loss [22]. In vitro, soluble factors from prostate cancer cells 'educated' OCys to promote tumor cell growth, migration, and invasion through changes in OCy secretome [23]. Conditioned media from multiple myeloma cells increased *rankl* and decreased *opg* expression in OCys as well as inhibited OCy cell growth [24]. Even fewer studies have investigated the impacts of tumor cells on OCys' ability to respond appropriately to mechanical stimuli, which is a significant gap in understanding how mechanical forces might be affecting TIBD. Fluid flow-induced changes in OCy expression of *rankl, opg,* and *rank:opg* were larger in the presence of media conditioned by multiple myeloma cells, seemingly sensitizing OCys to fluid flow [24]. In the case of breast cancer, we recently showed that the ability of OCys to mount an anabolic loading response while in the presence of tumor-conditioned media depended on whether the breast cancer cells themselves were also loaded [25]. When conditioned media was collected from loaded breast cancer cells, OCy cell counts were further reduced compared to static controls, and loading-induced increases in OCy *opg* were abrogated, leading to larger *rankl:opg*. However, these studies were conducted in 2D, which is not physiological, thus may not reflect a physiological OCy mechanoresponse.

Here, we sought to investigate how soluble factors secreted by breast cancer cells alter the mechanoresponse of OCys to fluid flow in a physiologically-relevant bone microenvironment. To this end, we developed a 3D OCy culture model and combined it with a perfusion bioreactor. We initially focused on applied perfusion with an established cell line, the highly fluid-sensitive MLO-Y4 OCys [26], in order to benchmark our results against existing literature. We then cultured MLO-Y4s with conditioned media collected from human breast cancer cells, as the majority of osteocytes are deeply embedded in the bone matrix, thus likely signal via paracrine signals. We utilized a highly aggressive human breast cancer cell line, MDA-MB-231s, and a corresponding subclone that specifically homes to bone to assess whether OCys responded differently to a subpopulation of tumor cells that exhibit osteotropism. Our rationale is that among breast cancer cells, which are highly heterogeneous, distinct gene and protein signatures exist that demarcate subpopulations and point to their preferred distant site (e.g., bone, lung, brain) [27] and likely lead to distinct impacts on the local osteocyte population. We collected conditioned media from both Parental and Bone-homing MDA-MB-231s across a range of tumor cell population sizes and assessed resulting MLO-Y4 growth and viability over time to identify appropriate culture parameters (i.e., time in culture and TCM dose) for subsequent experiments. Finally, using the determined culture parameters, we tested the impacts of tumor-conditioned media on the response of MLO-Y4s to applied perfusion to understand how tumor-derived paracrine signals impact osteocytes' mechanoresponse to fluid flow.

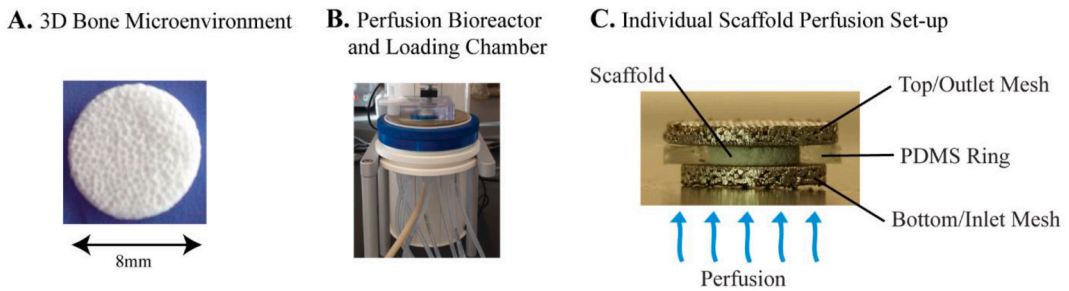

Fig. 1. 3D platform for osteocyte culture and perfusion bioreactor set-up. (A) Representative image of the bone-mimicking scaffold. **(B)** A single bioreactor chamber holds up to 9 scaffolds, each in individual wells, and is perfused from the bottom. **(C)** Each scaffold is surrounded by a PDMS ring to facilitate direct perfusion. A sintered mesh is placed below and above the scaffold/PDMS ring to create uniform inlet and outlet flows.

2. Materials and methods

2.1. Bone-mimicking scaffold fabrication

Bone-mimicking scaffolds were prepared from poly (lactide-*co*-glycolide) (PLG) and hydroxyapatite (HA) using previously established methods (Fig. 1A) [28,29]. Briefly, 8 mg of PLG microspheres, 8 mg of HA particles (Sigma, average diameter 200 nm), and 152 mg of NaCl particles sized 250–400 μm (J T. Baker) were pressure-molded (Carver Press) into disks (1.5 mm thick, 8 mm diameter). These disks were subsequently subjected to a gas-foaming/particulate leaching technique that results in surface exposure of the incorporated mineral.

2.2. 3D culture of MLO-Y4 osteocytes

MLO-Y4 cells (Kerafast) were selected as our OCy model when investigating the role of mechanical loading because their mechano-response to applied fluid shear stress is robust and well-characterized [26,30–32]. MLO-Y4s were cultured on collagen-coated tissue culture plastic [rat-tail collagen I (Fisher #CB-40236) diluted to 0.15 mg/ml in sterile 0.02 N acetic acid], and were maintained in Minimum Essential Medium Eagle – Alpha Modification (αMEM) supplemented with 2.5% fetal bovine serum (FBS, Life Technologies), 1% Penicillin/Streptomycin (P/S, Invitrogen) and 2.5% calf serum under standard cell culture conditions (37 °C, 5% CO_2). After MLOs reached ~70% confluency, they were detached with Trypsin-EDTA (Gibco) prior to scaffold seeding. Scaffolds were incubated with 70% ethanol for 30 min, washed 4× with sterile PBS, and then seeded with 500,000 MLO-Y4s per scaffold. MLO-seeded scaffolds were maintained on an orbital shaker at 37 °C and 5% CO_2 for 2 days prior to initiation of experiments to allow for cell adhesion and equilibration. Media changes were every 48 h unless otherwise described.

2.3. Generation of tumor-conditioned media

MDA-MB-231 (MDAs, ATCC) human breast cancer cells (Parental) and an MDA bone-homing (Bone-homing) subclone (a gift from Dr. Julie Rhoades, generated following an in vivo selection technique [27,33]) were maintained in complete Dulbecco's modified Eagle medium [DMEM (Invitrogen) supplemented with 10% FBS and 1% P/S] under standard cell culture conditions. To generate tumor-conditioned media (TCM), media was collected from a range of Parental and Bone-homing MDA cell populations (1e6, 4e6, 7e6, and 10e6 cells). MDAs were plated in tissue culture flasks, and when they reached 90% confluency, their media was replaced with low serum DMEM (1% FBS, 1% P/S) for 24 h. Cells were counted following trypsinization, and the total volume of TCM was aliquoted according to the desired population counts. For example, to generate aliquots of TCM from 10e6 cells, the total number of cells in a single T150 flask was divided by 10e6 to calculate the total number of aliquots. The 25 mL of TCM from the T150 was then divided by the total number of aliquots. Each aliquot received fresh low serum DMEM for a final volume of 15 mL. Each 15 mL aliquot of TCM was then condensed to 1.5 mL in an Amicon centrifugal filter unit (MWCO 3 kDa, EMD Millipore), and diluted as described previously [25,28,29] to achieve a final ratio of 20% TCM to 80% fresh MLO-Y4 media. TCM generated using this method has previously affected MLO-Y4 mechanosensitivity [25], osteogenic differentiation in mesenchymal stem cells [28], and osteoclastogenesis in RAW264.7 monocytes [29]. Low serum DMEM with no cells was subjected to the same processing conditions and used as acontrol.

2.4. Perfusion bioreactor

We first tested the MLO-Y4 response to steady versus pulsatile flow. Our rationale is that, when broadly looking across bone tissue engineering studies (i.e., 3D), particularly those that employ perfusion, they most often use steady flow. Thus, even though nearly all 2D MLO-Y4 studies employ unsteady flow, we opted to test whether there was a substantial difference in flow profiles. MLO-Y4-seeded scaffolds received either steady perfusion (0.3 ml/min inlet volumetric flow rate, resulting in 100 μm/s inlet velocity; 1 h per loading bout) or pulsatile perfusion (0.3 ml/min inlet volume applied at 1 Hz) from our bioreactor (Bangalore Integrated System Solutions) (Fig. 1B), loading regimes that we previously verified via Computational Fluid Dynamics simulations to be within the physiological range of anabolic mechanical loading [34,35]. Within the bioreactor chamber, each scaffold sits in an individual well (up to 9 per chamber), and is positioned between two sintered metal mesh disks that produce uniform inlet and outlet flows (Fig. 1C). To produce direct perfusion through scaffolds, each scaffold is also surrounded by a deformable PDMS ring that restricts outward flow from surrounding the sidewall (Fig. 1C).

2.5. Endpoint analyses

To assess overall MLO-Y4 population growth in 3D, DNA was isolated with Caron's buffer and quantified via analysis of fluorescence intensity using Quantifluor (Promega). To assess cell viability, live cells were stained with calcein and dead cells were stained with propidium iodide. Finally, to assess the mechanoresponse of MLO-Y4s in 3D, expression of *rankl* and *opg* was determined using quantitative RT-PCR (qPCR) and the comparative ΔCT method. Briefly, mRNA was isolated from scaffolds using the TRIzol extraction method in RNase-free conditions. qPCR was performed using Taqman probes and SYBR primers. Results were normalized to the expression of *hprt*, the housekeeping gene we determined to be invariant to all of our treatments. Details can be found in the supplement (Supplemental Table 1).

2.6. Statistical analysis

The effects of: 1) perfusion alone [Loaded (Steady and Pulsatile) vs. Nonloaded]; 2) TCM source (Control, Parental, or Bone-homing) and dose (1, 4, 7, and 10e6 tumor cells); 3) TCM source (Control, Parental, or Bone-homing), dose (1 vs. 4e6 cells), and day (D1, D3, and D5); and finally 4) TCM source (Control or Bone-homing) and perfusion (Loaded vs. Nonloaded) were determined via full factorial ANOVA (JMP Pro v16.0, SAS Institute Inc. and Rstudio: Integrated Development for R). When the interaction factor was significant, a post hoc Tukey-Kramer test with a Bonferroni correction was conducted; otherwise, experimental groups were pooled for analysis as appropriate to evaluate the main effects. All experiments were replicated 3–4 times, with a minimum of 3 technical replicates per treatment group per outcome measure. Outliers were identified via the Cook's Distance method. Data are represented as the mean ± SD across all biological replicates. Each data point represents the mean value from a single biological replicate. Statistical significance was set at $\alpha < 0.05$.

3. Results

3.1. MLO-Y4s developed interconnecting dendrites and exhibited a normal loading response to perfusion in a 3D bone microenvironment

After 7 total days of culture, MLO-Y4s remained widely viable throughout the scaffold. A representative image of a live/dead stain shows widespread dendrite formation and interconnections among neighboring cells (Fig. 2A). We also applied both steady and pulsatile fluid flow to MLO-Y4-seeded scaffolds to assess changes in expression of classic mechanosensitive remodeling genes – *rankl* and *opg* [36]. Perfusion was applied for 1 h per day for 2 consecutive days, based on documentation of temporal loading-induced changes to gene expression in vivo [37] as well as numerous 2D studies (NB: the reader is referred to several representative papers [24,38–41]) (Fig. 2B). Interestingly, MLO-Y4s in 3D were more responsive to a steady flow profile than to an unsteady one, as indicated by the remodeling rheostat *rankl:opg* ratio. Specifically, *rankl* was decreased by steady loading by 45%, but not by pulsatile flow ($p = 0.007$). Gene expression of *opg* followed a trend for a loading-induced increase in both flow conditions compared to static controls, but these changes did not reach significance ($p = 0.2$) (Fig. 2C). As a result, the ratio of *rankl:opg* was strongly reduced by flow ($p = 0.0002$), and it was not different between steady and pulsatile flow conditions. Thus, we selected steady flow for the remainder of our studies.

3.2. MLO-Y4 growth and viability in 3D was inhibited by conditioned media from bone-homing MDA-MB-231 breast cancer cells

To first determine how culture with tumor-conditioned media (TCM) impacted MLO-Y4 growth and viability in 3D, we cultured osteocytes with media conditioned by increasing the size of tumor cell populations (1, 4, 7, and 10e6 cells) (Supp. Fig. 1A). Upon inspection of the live/dead staining, however, MLO-Y4 cultures treated with Bone-homing TCM displayed a striking loss of cellularity

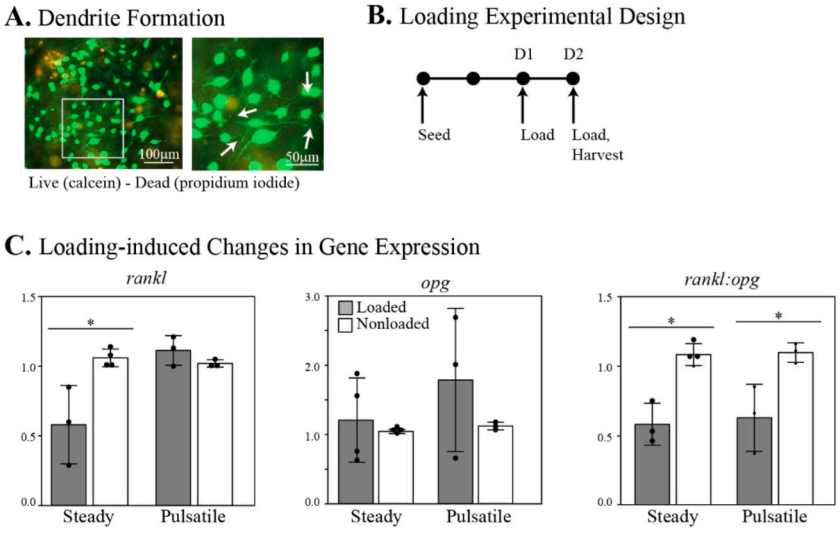

Fig. 2. MLO-Y4s in a 3D bone microenvironment recapitulated a physiologic mechanoresponse. **A)** MLOs in HA-containing scaffolds formed interconnecting dendrites (white arrows), as observed by live (calcein, green)/dead (propidium iodide, red) staining after 7 days in culture (representative image shown). Bar = 100 μm; inset bar = 50 μm. **B)** Experimental design schematic to test 3D MLO mechanoresponse to applied steady or pulsatile (1 Hz) perfusion (100 ml/min, 1 h per day, 2 days). **C)** *Rankl* was reduced only in MLO-Y4s exposed to steady perfusion. MLO-Y4s reduced their *rankl:opg* in response to both steady and pulsatile perfusion, with no difference in the loading response to either loading condition. A trend for loading-induced increases in *opg* expression was observed in both loading conditions, which did not reach significance. Each data point represents the mean value from each biological replicate (n = 3–4). *Loaded vs. Nonloaded via 2-way ANOVA.

with increasing TCM dose (Suppl. Fig. 1B). Concomitant with this, differences in overall MLO-Y4 growth were observed across the source of TCM, in which MLO-Y4 DNA content in cultures treated with Bone-homing MDA TCM was lower than that in the Control group and in the group treated with Parental MDA TCM. These differences did not reach statistical significance given the large variability in data; however, the level of genetic material in the MLO-Y4s treated with Bone-homing MDA TCM was so low, as shown by the absolute value of DNA content, that further endpoint analyses (e.g., qPCR) were precluded (Supp. Fig. 1C). Similarly, when MLO-Y4 DNA content was normalized to the Control group (Supp. Fig. 1D), the rate of growth in the MLO-Y4s treated with Bone-homing TCM was severely stunted. Because the higher doses of Bone-homing TCM limited the cellular material we could work with, we next investigated the temporal impacts of the lower TCM doses.

Because we observed significant loss in MLO-Y4 cellularity following 5 days of culture with higher doses of Bone-homing TCM (i.e. 7e6 and 10e6 cells), we sought to characterize temporal changes in MLO-Y4 net growth upon culture with the lower doses of TCM (i.e. 1e6 and 4e6 cells) (Fig. 3A). MLO populations overall on Days 3 and 5 were significantly larger than those of Day 1 ($p = 0.021$) (all TCM treatment and Control biological replicates pooled for each day), indicating initially net growth occurred and then tapered (Fig. 4B). The Control MLO-Y4s reached the largest population size after 5 days of culture compared to all other treatment groups. Additionally, overall population growth was significantly impacted by the source and dose of TCM treatment (Fig. 3B). MLO-Y4 populations treated with 1e6 Parental TCM as well as 1e6 Bone-homing TCM all had similar growth trajectories, in which their growth plateaued by Day 3 of culture. However, on Day 5, MLO-Y4 populations with the 4e6 dose of Bone-homing TCM reverted back to levels seen at Day 1. Taken together, MLO-Y4s were most impacted by TCM from the Bone-homing MDA variant, thus, in our

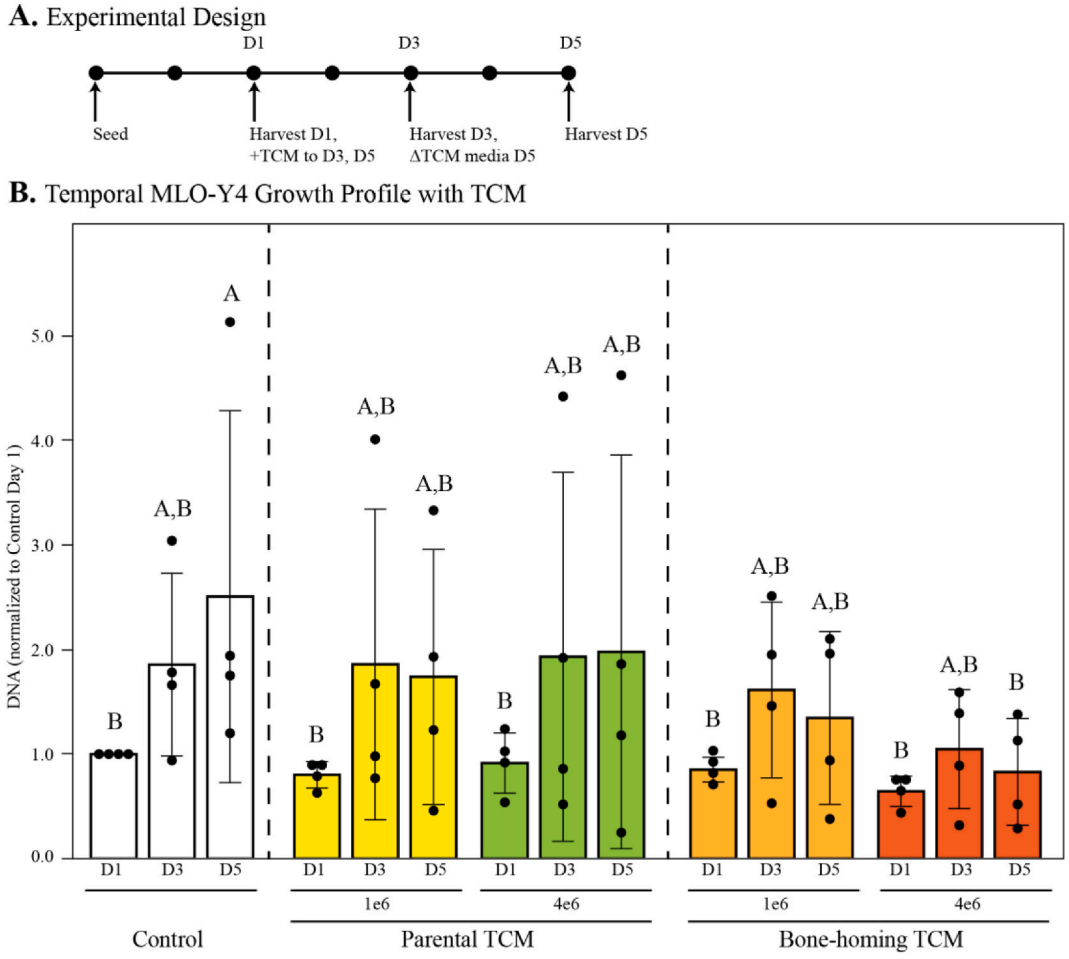

Fig. 3. Temporal MLO-Y4 growth and viability in 3D were impaired most by culture with media conditioned by Bone-homing MDA-MB-231 breast cancer cells. A) Experimental design schematic to assess temporal MLO-Y4 growth and viability in 3D with exposure to tumor-conditioned media (TCM) from Parental and Bone-homing MDAs. **B)** After 1, 3, and 5 days of culture with TCM, overall growth of MLO-Y4 populations receiving Parental MDA TCM was significantly smaller than that of Control MLO-Y4 populations, as indicated by total DNA content. MLO-Y4 populations receiving Bone-homing MDA TCM, particularly the 4e6 dose, was further diminished. Data from all replicate experiments pooled together. All control groups pooled together, as they received the same media. Same letters (A or B) indicate similar mean values, and groupings with different letters indicate that the difference is significant by post hoc comparison of means following a full-factorial ANOVA [factors: treatment group (Control, 1e6 Parental TCM, 4e6 Parental TCM, 1e6 Bone-homing TCM, 4e6 Bone-homing TCM), Day (D1, D3, D5)].

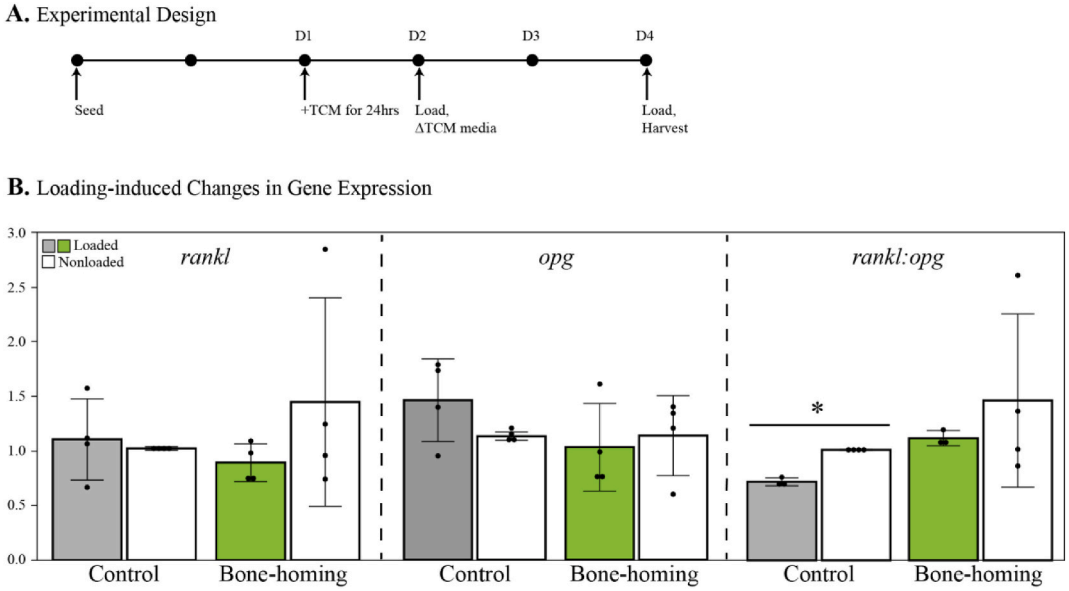

Fig. 4. The mechanoresponse of MLO-Y4s to applied perfusion was diminished by culture with media conditioned by MDA-MB-231 breast cancer cells. A) Experimental design schematic to assess the impacts of tumor-conditioned media (TCM) from Bone-homing MDAs on MLO-Y4 expression of bone remodeling genes. MLO-Y4s were cultured with the 1e6 TCM dose from Bone-homing MDAs, and also received 2 bouts of applied perfusion. **B)** While *rankl* and *opg* individually were unchanged by experimental treatments, *rankl:opg* was insensitive to loading in the MLO-Y4s receiving Bone-homing MDA TCM, with no significant loading-induced decreases occurring in TCM treated MLOs. Data from all replicate experiments was pooled together. *Loaded vs. Nonloaded via 2-way ANOVA.

subsequent fluid flow experiments, we focused on that TCM treatment. Furthermore, we selected the 1e6 TCM dose and a 4-day culture period to balance TCM-induced alterations to gene expression with significant drops in MLO-Y4 cellularity.

3.3. MLO-Y4 mechanoresponse was diminished with exposure to conditioned media from Bone-homing MDA-MB-231 breast cancer cells

Next, we tested the impact of the lowest TCM dose (i.e., media conditioned by 1e6 tumor cells) from the Bone-homing variant on the mechanoresponse of MLO-Y4s (Fig. 4A). To explore this, we added Bone-homing conditioned media 24 h prior to the onset of loading to ensure the TCM would affect the osteocytes prior to treatment with loading. We analyzed gene expression data for key osteocyte markers *rankl, opg,* and the *rankl:opg* ratio. (Fig. 4B). Following applied perfusion during culture with MDA TCM, the mechanoresponse of MLO-Y4s was modified relative to Control populations. While *rankl* expression was greatest in the Nonloaded group receiving Bone-homing MDA TCM, it was not significant. Expression was largely unchanged across all other treatment groups. Similar to our loading-alone results, *opg* expression was greatest in the loaded Control MLO-Y4 population, but this upregulation did not reach significance relative to both the Bone-homing TCM MLO-Y4 population as well as the Nonloaded Control population. However, *rankl:opg* was significantly increased for the MLO-Y4 population cultured in Bone-homing MDA TCM compared to the Control group ($p = 0.038$). Finally, mechanical loading reduced *rankl:opg* in the loaded Control population relative to the Nonloaded Control population.

4. Discussion

To study the impacts of bone metastatic breast cancer on osteocyte mechanobiology, we developed a novel 3D culture platform using a bone-mimetic scaffold and a perfusion bioreactor. In the current study, we focused on how bone metastatic breast cancer cells (MDA-MB-231s), including a bone-homing variant, impact osteocyte function. We showed that conditioned media from the MDA-MB-231 bone-homing subclone was more detrimental to MLO-Y4 growth and viability than that from Parental MDA-MB-231 cells, and the deleterious impacts were more pronounced with longer culture periods and larger doses of tumor-conditioned media. We then studied the impact of low-dose conditioned media on the response of MLO-Y4s to applied perfusion, and determined that loading-induced changes to *rankl* and *rankl:opg* gene expression were altered by culture with tumor-conditioned media.

In our scaffold, MLO-Y4 osteocytes remained viable and formed interconnecting dendrites, a result that is similar to other existing 3D osteocyte culture systems, including MLO-Y4s in hydrogels [42,43], IDG-SW3s in hydrogels [44–46], and OCY454s in collagen-coated polystyrene scaffolds [47]. One limitation of our work is that we utilized early-stage osteocytes, MLO-Y4s, rather than mature, late-stage osteocytes, such as IDG-SW3s [48], OCY454s [47], or primary osteocytes [49,50]. We chose the MLO-Y4 cell line, which has been extensively documented as being highly sensitive to fluid flow, so that we could benchmark our 3D results. In response to 2D unsteady fluid flow, MLO-Y4s readily increased their OPG expression [24,38–41] and decreased their *rankl:opg* [24,38,41,51,

52], similar to our current results and to what occurs physiologically [36]. Changes to *rankl* in 2D using unsteady flow, however, have been more mixed (increased: [38,39,41]; decreased: [40]; no change: [24]). In our hands, steady flow reduced *rankl* and *rankl:opg,* while pulsatile flow did not. In contrast, pulsatile flow, but not steady flow, only modestly increased *opg.* This potentially warrants future investigations to untangle the underlying reasons for the disparate response. Given that our goal is to test the effects of breast cancer on osteocyte mechanosensitivity and that most bone tissue engineering studies utilize steady perfusion, we opted to utilize steady perfusion in our subsequent cancer-related studies. In 3D, the response of osteocytes to applied loading has also been mixed. MLO-Y4s undergoing a shearing stress did not alter their *opg* or *rankl:opg* expression [42]. Mechanical unloading (via rotary bioreactor or suspension) of MLO-Y4s in 3D downregulated differentiation genes (e.g., *e11, dmp1*) [43]. Similarly, OCY454s increased *rankl* expression following unloading [47]. Interestingly, MLO-Y4s in our scaffolds were more responsive to steady flow than pulsatile fluid flow, and responded primarily through reductions in *rankl* expression. Physiological fluid flow, particularly in bone, is unsteady. Our results using MLO-Y4s might be explained by different cell morphologies between 2D and 3D. Cells are arranged in monolayers in 2D, and become polarized, which does not happen in vivo. In 3D, osteocytes have the freedom to form dendrites in any direction, and may exhibit a bridging morphology that elicits a different response than that of a flat morphology [53]. Additionally, cells in 2D flow studies, such as in a parallel plate flow chamber, uniformly experience the same shear stress profile, which is beneficial for controlling experimental factors, even if it is non-physiological. In our scaffold, the wall shear stress distribution is variable, which could account for a less strong mechanoresponse from our MLO-Y4 population. One approach to increasing the loading signal could be to increase the flow rate in the future. Nevertheless, our scaffold supported the formation of interconnecting MLO-Y4 osteocyte dendrites as well as an appropriate mechanoresponse. Future efforts will include translating this platform for use with late-stage osteocytes and primary osteocytes to enhance its physiological relevance.

While osteocytes in our 3D scaffold responded as expected to applied perfusion, our scaffold lacks a true lacunar-canalicular network, which could result in a different mechanoresponse compared to osteocytes within their native environment. To help mitigate this limitation, we have verified that the internal wall shear stresses resulting from our perfusion regime (0.3 ml/min inlet flow, resulting in 100 μm/s inlet velocity) are in the physiological range (~80% of values fell between 1 and 100 mPa; median = 10 mPa) via full-scale computational fluid dynamics modeling [34]. While these values are lower than those typically applied to MLO-Y4s in 2D [i.e. 1 Pa peak shear [24,38–41]], we successfully stimulated an anabolic response with perfusion. Future work should include verifying other known characteristic loading responses, such as a magnitude dose response. Additionally, more work will be needed to assess cellular attachment to the scaffold as well as the functionality of the dendrites, such as whether hemichannels form, particularly given their protective role against metastasis [19,54]. It is possible that culturing mature, matrix-producing osteocytes for sufficiently long periods will form their own lacunar-canalicular network within the scaffold [55,56], overcoming the limitations of our engineered scaffold.

The vast majority of investigations on the relationship between osteocytes and bone metastatic tumor cells have focused on the impacts that osteocytes have on breast cancer cell function, and the impacts of mechanically-stimulated osteocytes on tumor cell function are unclear. Conditioned media from stimulated osteocytes increased [18] or decreased [12,19] breast cancer cell proliferation, and increased [12,18] or decreased [19,57,58] breast cancer cell migration. Our goal, in contrast, was to investigate how tumor cells impact osteocytes, specifically their mechanoresponse, as a novel mechanism of tumor-induced bone disease. Others have reported that many bone metastatic cancers, including prostate [23],melanoma [21], and multiple myeloma [20,22,24], are correlated with altered functions of osteocytes (e.g., their secretome). These results suggest that their mechanoresponsiveness would also be impacted, but few studies have investigated this explicitly. Using 2D see-saw rocking, we previously showed when Parental MDA-MB-231 breast cancer cells were also loaded, their conditioned media caused osteocytes to have a limited mechanoresponse [25]. In the future, the impacts of loaded cancer cells should be tested in our 3D osteocyte system as well. In a recent study by the You group, MLO-Y4s treated with conditioned media from (Parental) MDA-MB-231s showed significant decreases in cellularity with modest increases in apoptosis [57]. These results differ from ours, where we show that conditioned media from Parental MDA-MB-231s does not impact MLO-Y4 cellularity, while conditioned media from Bone-homing MDA-MB-231s decreases cellularity. This could be due to dimensionality, where the MLO-Y4s might behave differently when cultured in 3D as opposed to 2D. It is also possible that differing conditioned media formulations might cause discrepant effects on osteocyte cellularity. Specifically, our tumor-conditioned media constitutes 25% of the total media volume(I.e., 25% conditioned media, 75% MLO-Y4 growth media), while the previous study utilized a 50:50 formulation. From the same group, MLO-Y4s and MDA-MB-231s were co-cultured and treated with low-magnitude high frequency (LMHF) vibration, and LMHF-activated osteocytes reduced overall cancer extravasation. Further, combined treatment with Yoda1, an activator of the mechanosensitive Piezo 1 channel, increased osteocyte mechanoresponsiveness via increased Ca^{2+} response despite breast cancer cell presence [57,58]. Key differences between the present study and theirs include that we estimated osteocyte mechanoresponsiveness via different endpoint measures, and the present study focused on a bone-homing sub-clone rather than the Parental MDA-MB-231 line. In the context of multiple myeloma, another osteolytic cancer, conditioned media was collected from either multiple myeloma cells or MLO-Y4 cells, which was then used to culture MLO-Y4s undergoing 2D fluid flow [24]. Contrasting with our results, the mechanoresponse of MLO-Y4s was increased with culture with multiple myeloma-conditioned media. Specifically, tumor-conditioned media stimulated not only greater overall *rankl* and less *opg* gene expression, but loading-induced changes to these genes were also larger. However, these results indicate that the specific type of cancer that has metastasized to the skeleton may have differing impacts on osteocytes. We also noted an inconsistency in *rankl* expression between our loading-alone and loading and conditioned media studies. The latter studies utilized concentrated tumor-conditioned media (DMEM) that was reconstituted in MLO-Y4 culture media (αMEM); the controls for tumor-conditioned media concentrated DMEM without any cancer cells. It is possible this difference in media compositions could cause a difference in *rankl* expressions. One possible way to overcome this is to apply a higher perfusion flow to increase the signal-to-noise ratio in gene expression. Taken together, these and our results support the

hypothesis that the osteocyte mechanosensing function is altered in response to breast cancer bone metastasis, and may constitute a novel mechanism of tumor-induced bone disease.

We observed a disparate response of osteocytes to soluble signals from Parental MDA-MB-231 breast cancer cells versus a bone-homing subclone created using an established in vivo selection technique [27,33]. Overall, this result was expected because primary breast cancer is a very heterogeneous disease, and successful metastasis to distant sites depends upon multiple cellular alterations and genetic programs that arise from the same tumor – that is, the two cell lines exhibit different behaviors [59]. More work is needed to further characterize the differences between the two cell lines in the context of osteocyte signaling and tumor progression. Additional studies should also investigate the impact of breast cancer subtype, which is classified based on hormone [estrogen (ER), progesterone (PR)] receptor and human epidermal growth factor receptor 2 (HER2) receptor status, because prognosis and therapy response are linked to subtype [60]. Here, we first investigated triple negative breast cancer because it has the poorest prognosis [1] and the highest metastasis rate after early breast cancer [61]. The MDA-MB-231 cell line is also commonly used to study breast cancer in vivo and in vitro. Despite clinical differences, bone is the predominant distant metastatic site for all subtypes, signifying the relevance of studying how various subtypes alter osteocytes and tumor-induced bone disease.

In conclusion, by establishing a new 3D in vitro system, we showed that osteocyte growth, viability, and mechanoresponse were impaired following culture with breast cancer-derived soluble signals. Further, we showed that a bone-homing subclone was more detrimental to osteocytes than its parental cell line.

5. Limitations of the study

There are currently several limitations to this study that future work should explore. First, MLO-Y4 osteocytes are early-stage osteocytes and do not express sclerostin as late-stage osteocytes do [26,62]. The results obtained utilizing this cell line, while valuable for comparing to previous studies of MLO-Y4s responding to loading, limit complete understanding of osteocyte-cancer cell interactions as the vast majority of osteocytes are mature and secrete sclerostin. Second, perfusion is widely documented to stimulate a pro-bone formation response in osteocytes (as reviewed elsewhere), thus the perfusion bioreactor is a suitable system to apply a mechanical load to cells cultured in a 3D platform. However, recent discoveries have called into question the dominance of fluid flow-based stimuli. For example, pores in which osteocytes reside behave as stress concentrations under matrix deformation, meaning the local strains are far higher and likely more important than originally estimated [63]. Additionally, we now know that osteocytes attach directly to their surrounding bone matrix [64], further implicating the importance of matrix strain [65]. Future work should investigate both perfusion and matrix strains, perhaps through applied compression, to more closely mimic physiology. The perfusion applied here was steady, though unsteady signals are required for bone remodeling in vivo. While we chose this regime based on an initial side-by-side comparison of steady versus pulsatile flow and on steady perfusion being more common in bone tissue engineering studies, future studies should employ unsteady flow. Lastly, a 3D system is more physiological than a 2D one, and we have extensively characterized the interior mechanics of our 3D bone scaffolds that attached cells would 'feel' during experimentation via computation modeling [34,35,66]. However, it does not mimic the native structure of the lacunar-canalicular network found within bone. Future studies could compare the performance of vitalized explants to scaffolds to evaluate any potential differences.

Author contribution statement

Blayne A. Sarazin: Conceived and designed the experiments; Performed the experiments; Analyzed and interpreted the data; Wrote the paper. Boyuan Liu, Elaine Goldman & Ashlyn N. Whitefield: Performed the experiments. Maureen E. Lynch: Conceived and designed the experiments; Analyzed and interpreted the data; Wrote the paper.

Data availability statement

Data will be made available on request.

Declaration of competing interest

The authors declare no conflict of interest with the contents of this article.

Acknowledgements

We thank Dr. Jeremy Keys for his help with live/dead imaging of MLO-Y4s. We thank Dr. William Thompson for his suggestions and edits of our Methods section. This work was supported by the National Science Foundation (NSF BMMB-2047187), the Cancer League of Colorado (Award #203445), and the Anschutz-Boulder (AB) Nexus. Publication of this article was funded by the University of Colorado Boulder Libraries Open Access Fund.

Appendix A. Supplementary data

Supplementary data to this article can be found online at https://doi.org/10.1016/j.heliyon.2023.e20248.

References

[1] R.L. Siegel, et al., Cancer Statistics, 2021, A Cancer Journal for Clinicians, CA, 2021 **n/a**(n/a).
[2] F. Saad, et al., Long-term efficacy of zoledronic acid for the prevention of skeletal complications in patients with metastatic hormone-refractory prostate cancer, J. Natl. Cancer Inst. 96 (11) (2004) 879–882.
[3] V. Grill, T.J. Martin, Hypercalcemia of malignancy, Rev. Endocr. Metab. Disord. 1 (4) (2000) 253–263.
[4] S.L. Dallas, M. Prideaux, L.F. Bonewald, The Osteocyte: an Endocrine Cell and More, Endocr Rev, 2013.
[5] M.B. Schaffler, et al., Osteocytes: Master Orchestrators of Bone, Calcif Tissue Int, 2013.
[6] M.E. Lynch, et al., Tibial compression is anabolic in the adult mouse skeleton despite reduced responsiveness with aging, Bone 49 (3) (2010) 439–446.
[7] T. Saarto, et al., Effect of supervised and home exercise training on bone mineral density among breast cancer patients. A 12-month randomised controlled trial, Osteoporos. Int. 23 (5) (2012) 1601–1612.
[8] K.M. Winters-Stone, et al., Impact + resistance training improves bone health and body composition in prematurely menopausal breast cancer survivors: a randomized controlled trial, Osteoporos, Int 24 (5) (2012) 1637–1646.
[9] R. Beaton, et al., Effects of exercise intervention on persons with metastatic cancer: a systematic review, Physiother. Can. 61 (3) (2009) 141–153.
[10] G. Sheill, et al., Considerations for exercise prescription in patients with bone metastases: a comprehensive narrative review, Pharm. Manag. PM R 10 (8) (2018) 843–864.
[11] D.A. Galvao, et al., Exercise preserves physical function in prostate cancer patients with bone metastases, Med. Sci. Sports Exerc. 50 (3) (2018) 393–399.
[12] Y. Fan, et al., Skeletal loading regulates breast cancer-associated osteolysis in a loading intensity-dependent fashion, Bone Research 8 (1) (2020) 9.
[13] M.E. Lynch, et al., In vivo tibial compression decreases osteolysis and tumor formation in a human metastatic breast cancer model, J. Bone Miner. Res. 28 (11) (2013) 2357–2367.
[14] G.M. Pagnotti, et al., Low intensity vibration mitigates tumor progression and protects bone quantity and quality in a murine model of myeloma, Bone 90 (2016) 69–79.
[15] M. Rummler, et al., Mechanical Loading Prevents Bone Destruction and Exerts Anti-tumor Effects in the MOPC315.BM.Luc Model of Myeloma Bone Disease, Acta Biomaterialia 119 (1) (2020) 247–258.
[16] N. Giuliani, et al., Increased osteocyte death in multiple myeloma patients: role in myeloma-induced osteoclast formation, Leukemia 26 (6) (2012) 1391–1401.
[17] E. Terpos, et al., Elevated circulating sclerostin correlates with advanced disease features and abnormal bone remodeling in symptomatic myeloma: reduction post-bortezomib monotherapy, Int. J. Cancer 131 (6) (2011) 1466–1471.
[18] Y.V. Ma, et al., Mechanical regulation of breast cancer migration and apoptosis via direct and indirect osteocyte signaling, J. Cell. Biochem. 119 (7) (2018) 5665–5675.
[19] J.Z. Zhou, et al., Osteocytic connexin hemichannels suppress breast cancer growth and bone metastasis, Oncogene 35 (43) (2016) 5597–5607.
[20] F. Ziouti, et al., An early myeloma bone disease model in skeletally mature mice as a platform for biomaterial characterization of the extracellular matrix, JAMA Oncol. 2020 (2020), 3985315.
[21] A. Sekita, et al., Synchronous disruption of anisotropic arrangement of the osteocyte network and collagen/apatite in melanoma bone metastasis, J. Struct. Biol. 197 (3) (2017) 260–270.
[22] J. Delgado-Calle, et al., Bidirectional notch signaling and osteocyte-derived factors in the bone marrow microenvironment promote tumor cell proliferation and bone destruction in multiple myeloma, Cancer Res. 76 (5) (2016) 1089–1100.
[23] W. Wang, et al., Prostate cancer promotes a vicious cycle of bone metastasis progression through inducing osteocytes to secrete GDF15 that stimulates prostate cancer growth and invasion, Oncogene 38 (23) (2019) 4540–4559.
[24] X. Wang, et al., Fluid shear stress increases osteocyte and inhibits osteoclasts via downregulating receptor-activator of nuclear factor kappaB (RANK)/Osteoprotegerin expression in myeloma microenvironment, Med. Sci. Mon. Int. Med. J. Exp. Clin. Res. 25 (2019) 5961–5968.
[25] W. Wang, et al., Mechanically-loaded breast cancer cells modify osteocyte mechanosensitivity by secreting factors that increase osteocyte dendrite formation and downstream resorption, Front. Endocrinol. 9 (2018) 352.
[26] L.F. Bonewald, Establishment and characterization of an osteocyte-like cell line, MLO-Y4, J Bone Miner Metab 17 (1) (1999) 61–65.
[27] Y. Kang, et al., A multigenic program mediating breast cancer metastasis to bone, Cancer Cell 3 (6) (2003) 537–549.
[28] M.E. Lynch, et al., Three-Dimensional mechanical loading modulates the osteogenic response of mesenchymal stem cells to tumor-derived soluble signals, Tissue Eng. 22 (15–16) (2016) 1006–1015.
[29] S.P. Pathi, et al., A novel 3-D mineralized tumor model to study breast cancer bone metastasis, PLoS One 5 (1) (2010) e8849.
[30] A. Fahlgren, et al., Supraphysiological loading induces osteocyte-mediated osteoclastogenesis in a novel in vitro model for bone implant loosening, J. Orthop. Res. (2017).
[31] R.T. Brady, F.J. O'Brien, D.A. Hoey, Mechanically stimulated bone cells secrete paracrine factors that regulate osteoprogenitor recruitment, proliferation, and differentiation, Biochem. Biophys. Res. Commun. 459 (1) (2015) 118–123.
[32] K. Middleton, et al., Microfluidic co-culture platform for investigating osteocyte-osteoclast signalling during fluid shear stress mechanostimulation, J. Biomech. 59 (2017) 35–42.
[33] I.J. Fidler, Selection of successive tumour lines for metastasis, Nat. New Biol. 242 (118) (1973) 148–149.
[34] B. Liu, et al., Perfusion applied to a 3D model of bone metastasis results in uniformly dispersed mechanical stimuli, Biotechnol. Bioeng. 115 (4) (2018) 1076–1085.
[35] B. Liu, et al., Multiphysics simulation of a compression-perfusion combined bioreactor to predict the mechanical microenvironment during bone metastatic breast cancer loading experiments, Biotechnol. Bioeng. 118 (5) (2021) 1779–1792.
[36] A.G. Robling, C.H. Turner, Mechanical signaling for bone modeling and remodeling, Crit. Rev. Eukaryot. Gene Expr. 19 (4) (2009) 319–338.
[37] S.M. Mantila Roosa, Y. Liu, C.H. Turner, Gene expression patterns in bone following mechanical loading, J. Bone Miner. Res. 26 (1) (2010) 100–112.
[38] L. You, et al., Osteocytes as mechanosensors in the inhibition of bone resorption due to mechanical loading, Bone 42 (1) (2008) 172–179.
[39] R.N. Kulkarni, et al., Mechanical loading prevents the stimulating effect of IL-1beta on osteocyte-modulated osteoclastogenesis, Biochem. Biophys. Res. Commun. 420 (1) (2012) 11–16.
[40] X. Li, et al., Connexin 43 is a potential regulator in fluid shear stress-induced signal transduction in osteocytes, J. Orthop. Res. 31 (12) (2013) 1959–1965.
[41] R.N. Kulkarni, et al., Inhibition of osteoclastogenesis by mechanically loaded osteocytes: involvement of MEPE, Calcif. Tissue Int. 87 (5) (2010) 461–468.
[42] Y. Takemura, et al., Mechanical loading induced osteocyte apoptosis and connexin 43 expression in three-dimensional cell culture and dental implant model, J. Biomed. Mater. Res. 107 (4) (2019) 815–827.
[43] R. Fournier, R.E. Harrison, Methods for Studying MLO-Y4 Osteocytes in Collagen-Hydroxyapatite Scaffolds in the Rotary Cell Culture System, Connect Tissue Res, 2020, pp. 1–18.
[44] R.L. Wilmoth, V.L. Ferguson, S.J. Bryant, A 3D, dynamically loaded hydrogel model of the osteochondral unit to study osteocyte mechanobiology, Adv. Healthcare Mater. 9 (22) (2020), e2001226.
[45] A.H. Aziz, et al., IDG-SW3 osteocyte differentiation and bone extracellular matrix deposition are enhanced in a 3D matrix metalloproteinase-sensitive hydrogel, ACS Appl. Bio Mater. 3 (3) (2020) 1666–1680.
[46] K. Chen, et al., High mineralization capacity of IDG-SW3 cells in 3D collagen hydrogel for bone healing in estrogen-deficient mice, Front. Bioeng. Biotechnol. 8 (2020) 864.
[47] J.M. Spatz, et al., The wnt inhibitor sclerostin is up-regulated by mechanical unloading in osteocytes in vitro, J. Biol. Chem. 290 (27) (2015) 16744–16758.
[48] S.M. Woo, et al., Cell line IDG-SW3 replicates osteoblast-to-late-osteocyte differentiation in vitro and accelerates bone formation in vivo, J. Bone Miner. Res. 26 (11) (2011) 2634–2646.
[49] A. Bernhardt, et al., Primary human osteocyte networks in pure and modified collagen gels, Tissue Eng. 25 (19–20) (2019) 1347–1355.

[50] J. Skottke, M. Gelinsky, A. Bernhardt, *In* vitro Co-culture model of primary human osteoblasts and osteocytes in collagen gels, Int. J. Mol. Sci. 20 (8) (2019).
[51] J.N. Zhang, et al., The role of the sphingosine-1-phosphate signaling pathway in osteocyte mechanotransduction, Bone 79 (2015) 71–78.
[52] J. Li, et al., Effect of oscillating fluid flow stimulation on osteocyte mRNA expression, J. Biomech. 45 (2) (2012) 247–251.
[53] C. Jungreuthmayer, et al., Deformation simulation of cells seeded on a collagen-GAG scaffold in a flow perfusion bioreactor using a sequential 3D CFD-elastostatics model, Med. Eng. Phys. 31 (4) (2009) 420–427.
[54] J.Z. Zhou, et al., Differential impact of adenosine nucleotides released by osteocytes on breast cancer growth and bone metastasis, Oncogene 34 (14) (2015) 1831–1842.
[55] W.R. Thompson, et al., Osteocyte specific responses to soluble and mechanical stimuli in a stem cell derived culture model, Sci. Rep. 5 (2015), 11049.
[56] R. Dhurjati, et al., Extended-term culture of bone cells in a compartmentalized bioreactor, Tissue Eng. 12 (11) (2006) 3045–3054.
[57] C.Y. Lin, et al., Yoda1 enhanced low-magnitude high-frequency vibration on osteocytes in regulation of MDA-MB-231 breast cancer cell migration, Cancers 14 (14) (2022).
[58] X. Song, et al., Reduction of breast cancer extravasation via vibration activated osteocyte regulation, iScience 25 (12) (2022), 105500.
[59] D.X. Nguyen, J. Massague, Genetic determinants of cancer metastasis, Nat. Rev. Genet. 8 (5) (2007) 341–352.
[60] R. Rouzier, et al., Breast cancer molecular subtypes respond differently to preoperative chemotherapy, Clin. Cancer Res. 11 (16) (2005) 5678–5685.
[61] M. Van Mechelen, et al., Behavior of metastatic breast cancer according to subtype, Breast Cancer Res. Treat. 181 (1) (2020) 115–125.
[62] L.F. Bonewald, The Amazing Osteocyte, J Bone Miner Res, 2011.
[63] D.P. Nicolella, et al., Osteocyte lacunae tissue strain in cortical bone, J. Biomech. 39 (9) (2006) 1735–1743.
[64] L.M. McNamara, et al., Attachment of osteocyte cell processes to the bone matrix, Anat. Rec. 292 (3) (2009) 355–363.
[65] Y. Wang, et al., Strain amplification and integrin based signaling in osteocytes, J. Musculoskelet. Neuronal Interact. 8 (4) (2008) 332–334.
[66] S. Han, et al., Flow inside a bone scaffold: visualization using 3D phase contrast MRI and comparison with numerical simulations, J. Biomech. 126 (2021), 110625.